Journal of Marine Research, 48, 319–333, 1990

Some features of the upwelling off Oman

by Alan J. Elliott[1] and Graham Savidge[2]

ABSTRACT

Hydrographic and ADCP data were collected in the coastal waters of Oman during the 1987 summer monsoon. The minimum surface temperatures, up to 5°C below ambient offshore values, were found close to the coast and in the vicinity of the Kuria Muria Islands. Strong surface gradients were observed near Ras al Hadd at the entrance to the Gulf of Oman where the geostrophic surface flow exceeded 1.0 m/s. The alongshore flux in the top 300 m of a region extending 100 km from the coast was estimated to be 10×10^6 m^3/s. Evidence for an offshore filament of cool water was found in both current and temperature data.

1. Introduction

The monsoon currents in the northern Indian Ocean form one of the most energetic current systems in the world, with the twice yearly reversals of the wind stress in the equatorial zones producing corresponding reversals in the upper ocean currents. During the SW monsoon, in the northern summer, strong upwelling occurs over a large area along the Somali and Arabian coasts. There has been considerable previous work on the observation and modelling of the response to the monsoon winds at low latitudes off the coast of Somalia (e.g. Warren *et al.*, 1966; Luther and O'Brien, 1985). In that region the Somalia Current develops from a weak southward flow to a strong northward one, with a transport of more than 80×10^6 m^3/s (Leetma *et al.*, 1982), within four months of the onset of the SW monsoon. Much effort has focused on the two gyre system that subsequently forms off the Somali coast, and summaries of the observational and theoretical advances have been given by Schott (1983) and Knox and Anderson (1985), respectively. Less attention has been paid to the response along the coast of Oman. Bruce (1974) has presented surface distributions of temperature and salinity collected during the International Indian Ocean Expedition in 1963, while Smith and Bottero (1977) used the same data set to estimate the geostrophic and Ekman currents and determine the absolute sea surface topography in a region extending out to 400 km from the coast of Oman. In contrast to the lower latitudes off

1. Unit for Coastal and Estuarine Studies, Marine Science Laboratories, Menai Bridge, Gwynedd LL59 5EY, United Kingdom.
2. Marine Biology Station, The Strand, Portaferry Co. Down, Northern Ireland.

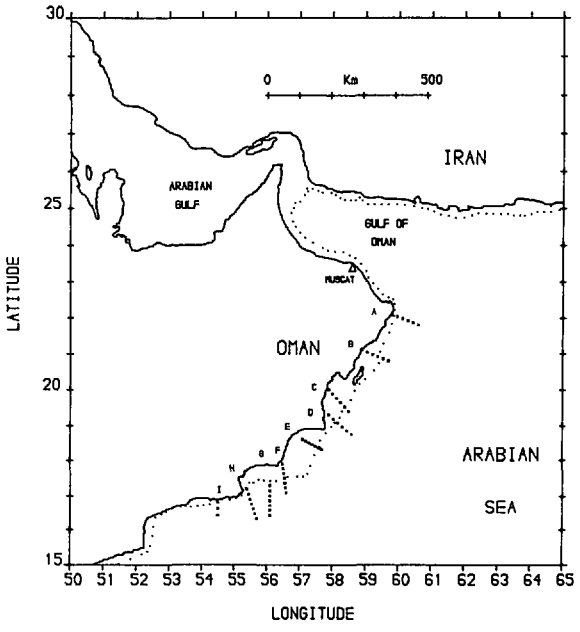

Figure 1. The northern Arabian Sea showing the transect positions off the SE coast of Oman; the 200 m isobath is shown by a dotted line.

Somalia there is a paucity of observations from the Omani waters, especially of current measurements but also of routine hydrographic data (Qasim, 1982).

In recent years, satellite images have provided evidence for a rich thermal structure in the upwelling region off Oman (e.g. Weaks, 1983). The images show regions of intense upwelling near headlands with filaments of cold water extending into the Indian Ocean and across the entrance to the Gulf of Oman. The upwelling regime has obvious implications for the fishing industry of Oman, and the associated current systems are relevant to local environmental issues. Parts of the coastline, especially those inshore of the Kuria Muria Islands (near position G, Fig. 1), are of special ecological interest and yet are adjacent to some of the world's busiest shipping routes. There is concern that a major oil spill, or similar maritime accident, could cause irreparable damage to sensitive areas. Consequently, there is an interest in the strength of the nearshore currents during the upwelling season, as well as the need to define the regions of intense upwelling near the coast.

During the summer of 1987 the RRS *Charles Darwin* was available for 10 days of ship time, sailing from the port of Muscat in the Gulf of Oman. Since the interest was in the nearshore regions, the survey grid extended from the coast out to 100 km with a nominal station spacing of 20 km (actually 10 nautical miles, 18.5 km). In most regions the shelf, with depths less than 200 m, is about 35 km wide except near the Kuria Muria Islands where the shelf extends out to 70 km. Off the shelf the depth increases

rapidly to reach a value of about 3,000 m. Thus the station grid spanned the shelf break region while concentrating on the nearshore areas. The purpose of the cruise was to map the distributions of temperature and salinity, dissolved oxygen and nutrients; a summary of the general distributions of these parameters is discussed in Savidge *et al.* (1990). The results described here concern features of the nearshore currents associated with the monsoon response.

Hydrographic and chemical data were collected along the station transects shown in Figure 1. Remote sensing images of earlier monsoons (Weaks, 1983 and Fig. 2) had suggested that the regions of intense upwelling would be located on the downstream side of headlands (near positions H, F, D; Fig. 1) and off Ras al Hadd at the entrance to the Gulf of Oman (position A, Fig. 1). Consequently, the station grid was designed so that data would be collected within and between the expected regions of intense upwelling. A hull-mounted ADCP was run continuously during the cruise with a vertical bin size of 8 m and an integrating period of 10 minutes. For each of the station positions a representative ADCP profile was selected from the group collected while the ship was on station, bottom tracking being used for stations on the shelf. The ADCP data from the surface bin were not used, instead the near-surface currents were estimated by averaging over bins 2 and 3. Since satellite coverage by the GPS positioning system was not sufficient to allow absolute current profiles to be determined a reference level of 300 m was used for estimating absolute currents in deep water. Surface temperature and fluorescence were monitored continuously from an inlet port in the hull at a depth of 4 m.

2. Results

Before discussing our observations and placing them in the context of the 1987 monsoon conditions, it is useful to examine some historical wind and current data from the Omani coastal waters. A pseudo-wind stress field for the Indian Ocean, consisting of monthly mean averages of the wind squared vector, has been derived by Florida State University (FSU) for the years 1977–1986 inclusive (Legler *et al.*, 1989). Figure 3 shows the 10-year average pseudo-stress computed by averaging the months of August. Near Masirah Island, at 20N 55E, the pseudo-stress has a magnitude of about 100 $(m/s)^2$ giving an estimate of about 10 m/s for the mean August wind speed. Although the FSU wind maps only present monthly averages of the stress field it is possible to use them to determine some seasonal characteristics of the wind regime off the coast of Oman. Following the NE monsoon winds, which blow during November–March, the onset of the SW monsoon is evident during April. The winds are then strong and steady during June–August, although they weaken considerably during September and reverse at the end of October. Fieux and Stommel (1977) analyzed daily ship reports of surface winds from the Arabian Sea and showed that the SW monsoon winds establish off the coast of Oman during early April within a time scale of about one

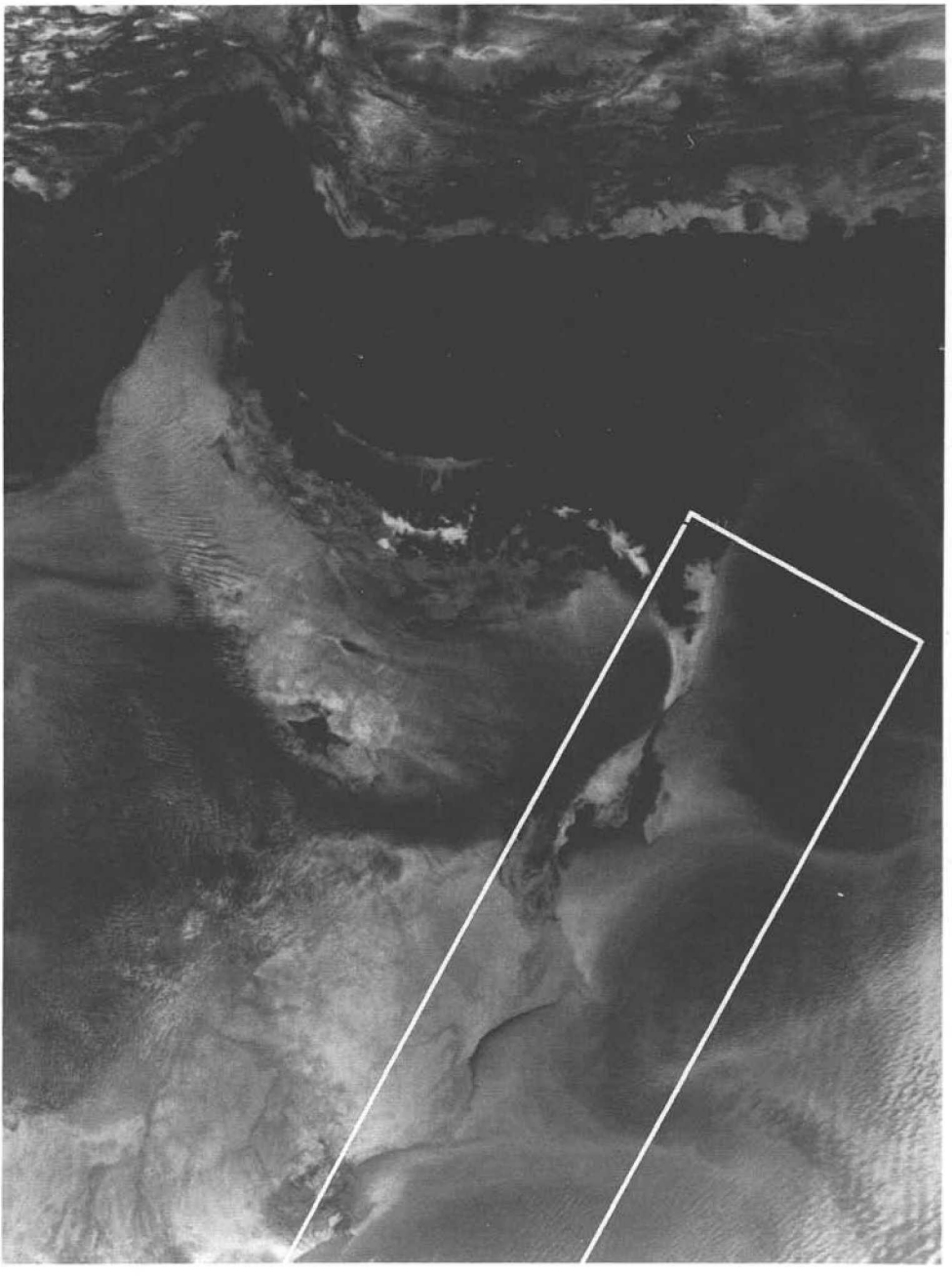

Figure 2. SST image of the Gulf of Oman and the Arabian Sea taken June 9 1985. The box shows the area in which data were collected during the 1987 cruise.

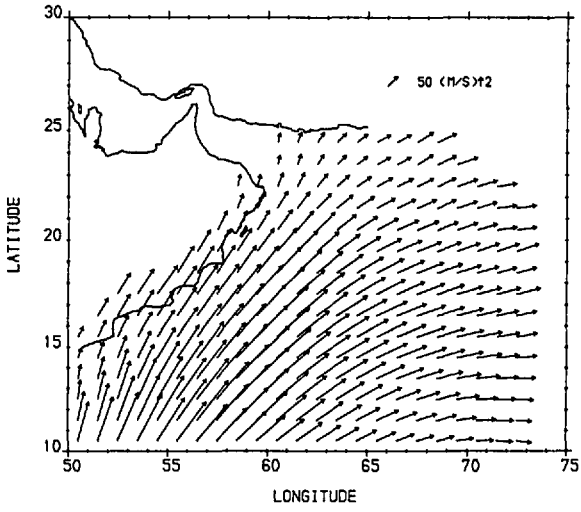

Figure 3. Mean August pseudo-stress computed by averaging over the years 1977–1986.

week. A strong correlation was found between the time of the monsoon onset and the subsequent rainfall along the west coast of India (Fieux, 1975).

During the summer of 1987 the winds recorded at Masirah, the island between sections B and C on Figure 1, had a mean speed of about 7 m/s (Fig. 4). Consequently the wind stress was around 50% of the 1977–1986 August mean. The mean daily winds showed a pronounced 20-day variability, ranging from peak values of about 12 m/s down to minimum speeds of around 3 m/s. The winds were relatively weak and from the south at the start of the cruise period (August 17–26). The global meteorological records from the Indian Ocean for the summer of 1987 suggest that the monsoon for that year was of a known type: the rains started late over India and a relative drought in the western areas during the early summer was balanced by heavy rain later in the NE

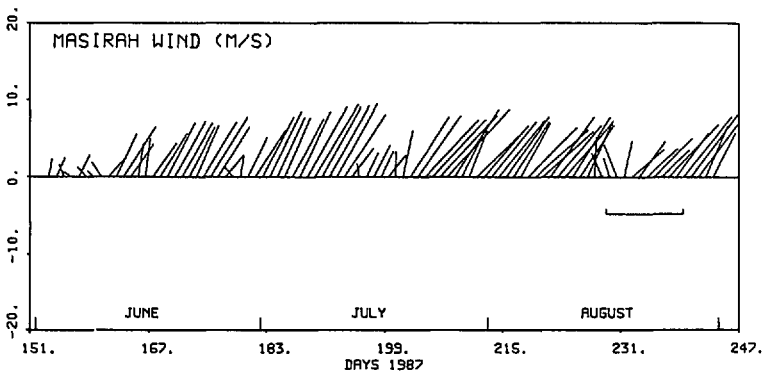

Figure 4. Wind (m/s) recorded at Masirah during the summer of 1987, the period of the cruise (August 17–26) is indicated.

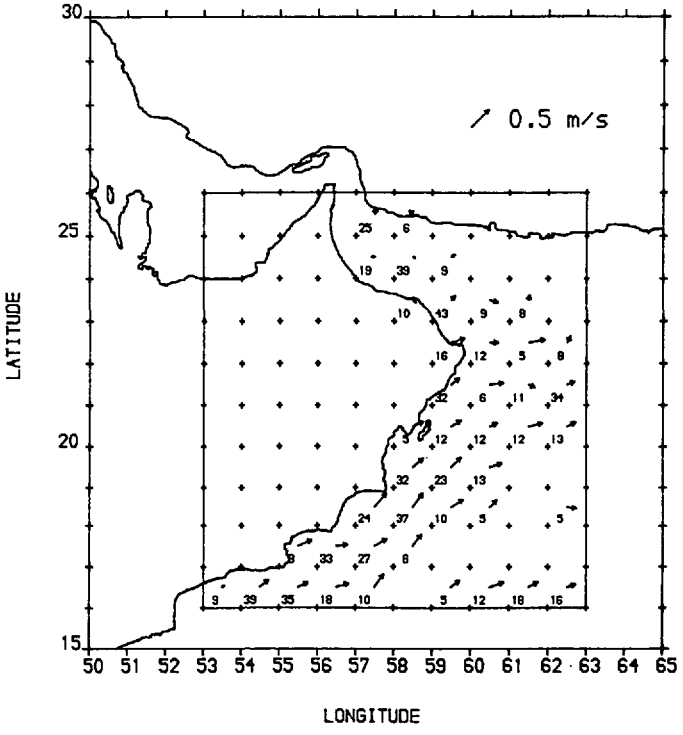

Figure 5. Mean surface currents (m/s) for the month of August derived from historical ship drift data. The numerals show the number of data points in each 1° × 1° box.

(S Gregory, pers. comm.). This is not a typical monsoon but it does fall into a recognized pattern (Gregory, 1988).

Historical information on the surface currents in the region can be derived from ship drift archives. In the 10° × 10° region covering 16–26N and 53–63E there are approximately 12,000 entries dating from the 1920's (M G Colgate, British Meteorological Office, pers. comm.). These data have been sorted by month into 1° × 1° boxes and the mean drift vectors for August are shown in Figure 5. The numbers represent the data count within each square, mean vectors have only been computed for squares containing more than 5 entries. Although data coverage is poor offshore there are about 30 data points in each of the near coastal squares. The data clearly show a NE flow of magnitude around 0.4 m/s extending to 200 km out from the coast. The drift data also suggest that the flow turns abruptly to the east off Ras al Hadd at the entrance to the Gulf of Oman. This can be contrasted with the mean wind field for August which shows a northeastward wind stress at the entrance to the Gulf. A more detailed analysis, in which the ship drift data were sorted in 10 day intervals, showed that the NE coastal current establishes off Oman toward the end of April soon after the winds start blowing to the NE. The drift data suggest that maximum currents occur toward the end of

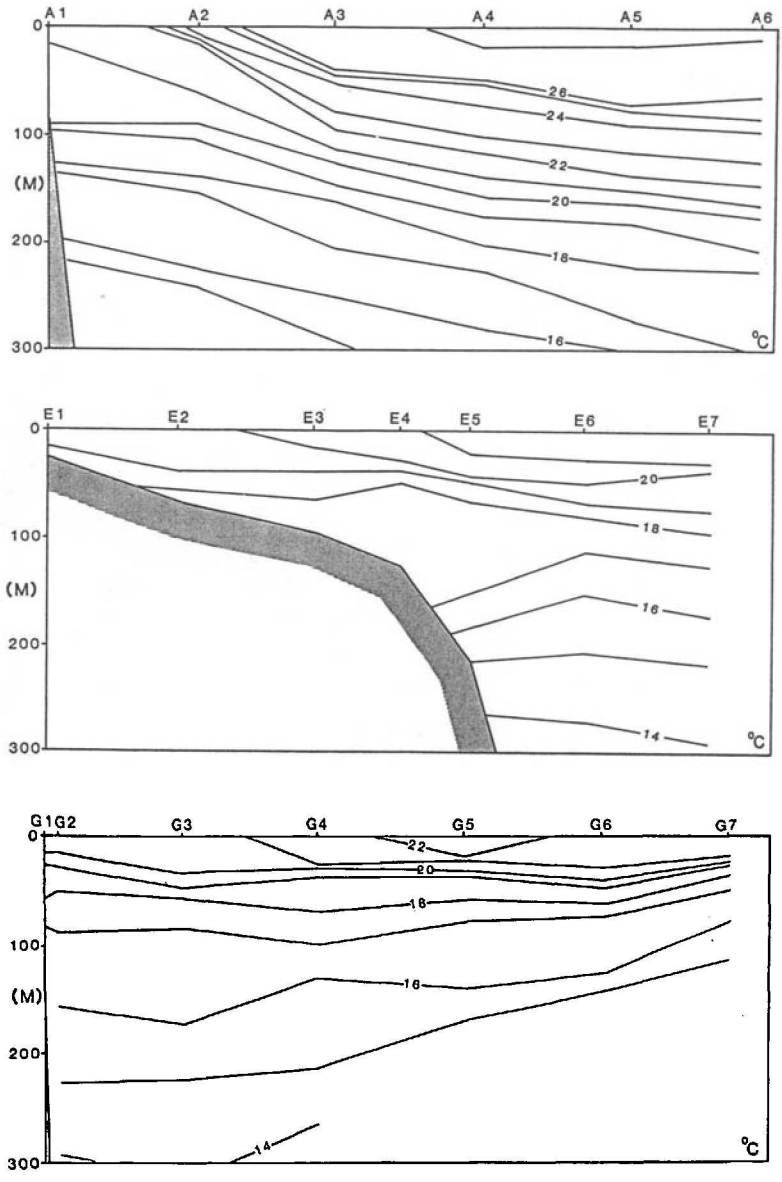

Figure 6. Vertical temperature sections (°C) at transects A, E and G.

June, that they hold steady during July and August, weaken during September and reverse around October 25.

Examples of the temperature sections are shown in Figure 6. At section A, near Ras al Hadd, surface temperatures in excess of 27°C were found offshore while the coastal waters had a surface temperature below 22°C. Near station A2 a temperature

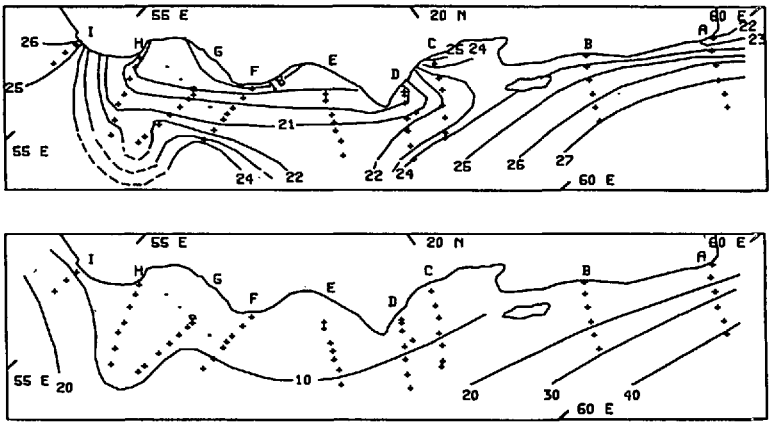

Figure 7. Top: Observed surface temperature distribution (°C). Bottom: Relative dynamic heights (cm) of the sea surface with respect to 500 m.

difference of about 5°C occurred over a distance of 25 km. Offshore there was a weak thermocline at depths of 60–70 m and a significant tilting of the isotherms at all depths above 300 m. Nearshore the isotherms were only tilted in the top 100 m. The temperatures were significantly lower at sections E and G, typical surface values being in the range 18–22°C. At both of these sections the strongest surface gradients occurred away from the coast, at E they were above the shelf break region and at G they were found at about 50 km offshore of the Kuria Muria Islands and consequently well offshore of the shelf break. In contrast to section A, isotherm tilting was not apparent at section G and was restricted to the upper 100 m at section E. At all sections the salinity structure was comparatively homogeneous and density was dominated by the effects of temperature (Savidge *et al.*, 1990).

The observed surface temperature distribution is shown in Figure 7 and can be compared with the satellite image of June 1985 (Fig. 2). The image shows cold cores, with temperatures around 18°C, near positions H, D and Masirah. Cool plumes, with temperatures of about 20°C, extend into the ambient surface waters which have a temperature of about 24°C. The regions of intense upwelling are confined to the downstream side of headlands, while warm water is shown inshore of Masirah and extending between positions B and C. The offshore jets, evident between E-F and near Masirah, had widths of about 55 km at distances of the order of 100 km from the coast. Some of these thermal features were reproduced in our observations. The maximum surface temperatures, in excess of 27°C, were found at the offshore end of section A. A *T-S* analysis suggests that this water originated within the Gulf of Oman (Savidge *et al.*, 1990). Warm water was found inshore of Masirah, between sections B and C, while the coldest water was located against the coast near position F. This cold pool of water had a temperature of about 18°C. There was a diffuse region of cool water (temperature around 19–21°C) between sections H and D, with the suggestion of a cold plume

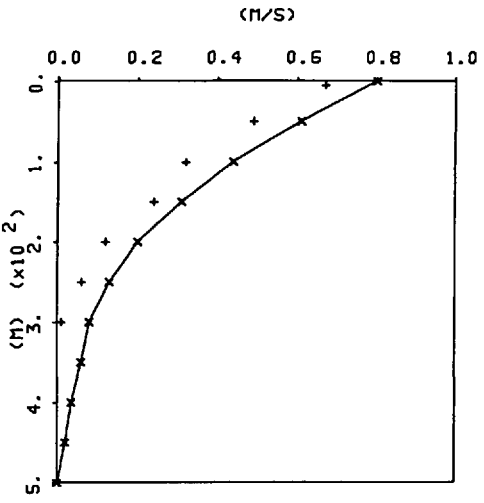

Figure 8. The geostrophic profile (solid curve) computed using the station data from A2 and A5, and the component of the ADCP profile directed through the section from station A3. The geostrophic current has a reference level of 500 m, the ADCP profile was referenced to 300 m.

extending offshore near section E. Warm surface water was encountered near section I, this water had similar *T-S* properties to the water found offshore of section A.

The dynamic height of the surface with respect to 500 m is also shown in Figure 7. Along section A there was a dynamic height difference of 0.20 dynamic m over a distance of about 65 km. Coupled with the low latitude, this produced a surface geostrophic flow of about 0.8 m/s (Fig. 8). The only other area in which the dynamic height showed a considerable gradient was along section I, elsewhere the gradients were relatively weak. Figure 8 shows the geostrophic current profile computed using the data from stations A2 and A5 (Fig. 6), also shown is the component of flow normal to the transect determined from the ADCP profile collected at station A3. The ADCP profile is referenced to 300 m, however a good agreement is obtained between the two profiles if the ADCP profile is offset by about 0.10 m/s at 300 m to make it match the geostrophic flow at that depth. The vertical geostrophic shear was strong in the upper 200 m, having a value of about 6×10^{-3} s^{-1}, decreased beneath 200 m and was weak below 300 m. Similarly strong geostrophic flow was computed across section I.

Table 1 shows the agreement between the geostrophic and ADCP currents normal to sections A and I. The ADCP profiles (underlined) are shown at the station positions with the geostrophic profiles, computed from the station pairs, shown between. In almost all cases offsetting the ADCP profile by the magnitude of the geostrophic flow at 300 m produces good agreement between the two data sets. The exception is the upper 100 m flow between stations A2 and A3 where the geostrophic flow was twice as strong as the flow recorded by the ADCP. However, this is the region of the strong surface front (Figs. 6–7) where the ageostrophic component of the flow may have been

Table 1. Geostrophic (m/s) and ADCP currents (underlined) through sections A and I; the geostrophic flow is referenced to 500 m, the ADCP currents to 300 m.

	A2		A3		A4		A5		A6
(m)									
0	0.46	1.16	0.67	0.62	0.51	0.61	0.38	0.35	0.28
50	0.25	0.67	0.48	0.57	0.46	0.59	0.46	0.35	0.22
10	−0.04	0.46	0.32	0.44	0.32	0.41	0.30	0.32	0.26
150	−0.21	0.26	0.23	0.35	0.18	0.32	0.20	0.27	0.18
200	−0.22	0.10	0.12	0.25	0.17	0.25	0.14	0.16	0.19
250	−0.14	0.04	0.05	0.15	0.10	0.20	0.02	0.07	0.13
300	0.00	0.02	0.00	0.08	0.00	0.15	0.00	0.02	0.00
350		0.02		0.04		0.11		0.00	
400		0.01		0.03		0.07		−0.01	
450		0.00		0.01		0.05		−0.03	
500		0.00		0.00		0.00		0.00	
			I1		I2		I3		
(m)									
0			0.66	0.70	0.74	0.45	0.47		
50			−0.09	0.33	0.61	0.41	0.33		
100			−0.02	0.07	0.13	0.21	0.17		
150			0.01	0.03	0.00	0.09	0.12		
200			−0.09	0.02	−0.02	0.03	0.05		
250			−0.01	0.02	0.01	−0.00	0.02		
300			0.00	0.04	0.00	−0.01	0.00		
350				0.04		−0.02			
400				0.05		−0.02			
450				0.03		−0.01			
500				0.00		0.00			

significant. The geostrophic calculations showed that the northeastward flow component weakened toward the SW (i.e. from A to H), and that the flow was weak and variable with southwesterly components near sections F, G and H. Strong flow was then encountered near section I in response to the increased offshore temperature gradient (Fig. 7). From Table 1 we can estimate the flux through section A as 10×10^6 m^3/s in the upper 300 m between the coast and 100 km offshore. This can be compared with the flux of 80×10^6 m^3/s estimated by Leetma *et al.* (1982) as the flux of the Somali Current in the upper 100 m. Smith and Bottero (1977) estimated the surface geostrophic currents in this region to be of magnitude 0.25–0.50 m/s and showed that the northeastward transport extended to 400 km out from the coast. Our data suggest that the strongest flows are to be found close against the coast (Table 1).

Maps of the ADCP current vectors at the near-surface, 100 m and 200 m are shown in Figure 9. The surface pattern shows strong northeastward (greater than 0.5 m/s) flow at sections A and I, and considerable offshore flow components at sections E-H. At section E the offshore stations showed a coherent pattern of flow away from the coast.

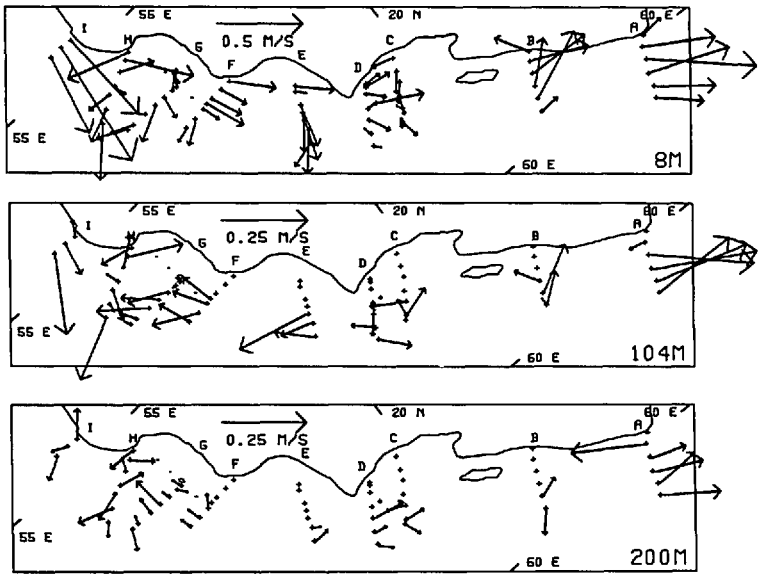

Figure 9. Maps of the ADCP current vectors at the near-surface, 100 m and 200 m. (Note the change of scale at the lower two levels.)

At sections B, C and H the flow was against the wind near the coast. The strong northeastward flow persisted at 100 m and 200 m at section A, consistent with the isotherm tilting shown in Figure 6. However, at many of the stations the flow at 100 m was directed against the wind. From a single survey it is not possible to separate the mean flow from oscillatory components such as tidal and inertial motions. However, we expect these components to be small since the tides are generally weak in the area (Admiralty Pilot, 1967), and since inertial motions are likely to be less than 0.02 m/s (based on a crude Pollard-Rhines-Thompson simulation).

The organized flow away from the coast at section E (Fig. 9, near surface) is consistent with the offshore extension of the isotherms shown in Figure 7. Figure 10 shows the vertical structure of the ADCP currents at stations E7-E3. At the offshore stations, especially E6, the offshore flow (toward the SE) was limited to the upper 100 m; closer inshore the flow was restricted to the top 50 m. During the return to Muscat the ship track crossed the position of this jet-like feature, and the surface temperature and ADCP vectors (with respect to 300 m) are shown at approximately 5 km intervals in Figure 11. These data were collected on August 25, four days after the original sampling at section E. Although there is some correlation between cool water with offshore flow, e.g. at points a and c, and warmer water with onshore flow, e.g. points b and d, there is no evidence for a simple offshore jet at section E, instead the current vectors show a complex pattern of on/offshore flow. At point c there was a region of offshore flow about 20 km wide, which contained speeds of about 0.30 m/s, this is comparable to the jet suggested by Figures 9–10. We can estimate the offshore

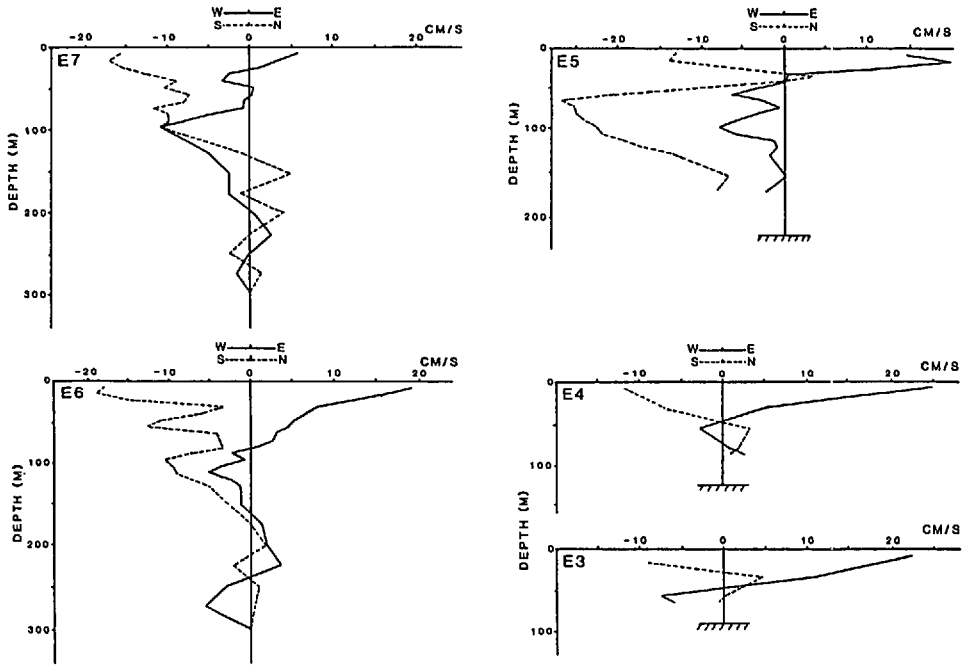

Figure 10. Vertical ADCP current profiles at stations E7-E3.

flux in this jet to be about 0.3×10^6 m^3/s which is only 3% of the estimated flow along the coast through section A.

3. Discussion

Remote sensing images (Weaks, 1983 and Fig. 2) have shown regions of intense upwelling close against the coast of Oman. This has been supported by our observations which detected the coldest water on the downstream side of a headland (near position F, Fig. 1) and a diffuse patch of cold water near the Kuria Muria Islands (sections G-H). There was at least a 5°C temperature difference between the regions of upwelled water and the ambient surface waters. Near Ras al Hadd, at the entrance to the Gulf of Oman (section A), and Ras Marbat, close to the border with South Yemen (section I), the surface waters had *T-S* characteristics similar to the water found within the Gulf of Oman. This water had a surface temperature in excess of 26°C. The strongest surface temperature gradients were found close to the coast near Ras al Hadd (section A) where there was a surface front with a temperature difference of 5°C over a distance of 30 km. There is probably a complex interaction at this point as the northeastward surface currents and upwelled water interact with the waters of the Gulf of Oman. The ship drift archive (Fig. 5) suggests that the surface flow turns abruptly to the east in the vicinity of Ras al Hadd.

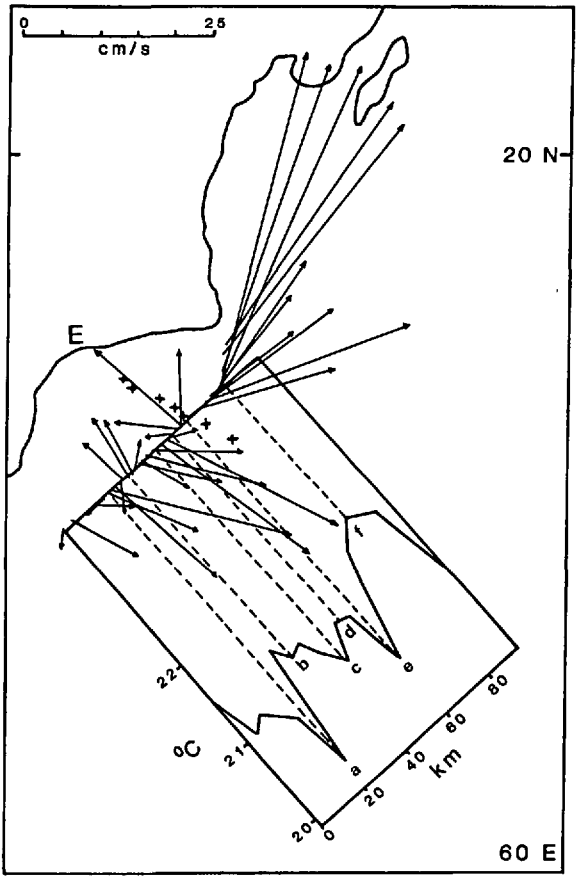

Figure 11. Surface current vectors and temperatures along the ship track when crossing the position of section E.

The nearshore geostrophic currents were strong, reaching speeds in excess of 1 m/s, and were in good agreement with the ADCP data. The alongshore flux in the top 300 m was estimated to be of the order of 10×10^6 m^3/s through section A which extended 100 km out from the coast. In the vicinity of the Kuria Muria Islands the surface flow was weak and showed a significant offshore component (Fig. 9). The suggestion of an offshore jet was found in the ADCP data from section E, this agreed with the offshore extension of the isotherms (Fig. 7) and the weak alongshore geostrophic flow at that location. The offshore transport of the cold filament was estimated to be about 3% of the flow through section A.

Since our data set is not extensive, it is instructive to compare it with results obtained in the upwelling zone off Oregon. In both regions the alongshore surface flow is directed with the wind, and a geostrophic balance exists between the alongshore flow and the pressure gradient associated with the offshore temperature differences. The Oregon

data sets have shown clear evidence for a counter-current directed against the wind at depths greater than 80–100 m. Kosro (1987) found the counter-current to be strongest at the shelf break, a feature that is possibly supported by our data (Figs. 6 and 9, station E5). In addition, Huyer and Kosro (1987) showed evidence of a countercurrent close to the coast, the flow being strongest within 5 km of the shore. This is compatible with the reverse surface flow found at stations B1, C1 and H1 (Fig. 9). Flament *et al.* (1985) observed a cold filament, extending away from the Oregon coast, that was 40 km wide and which advected surface water at speeds up to 0.5 m/s. The current speed within the jet decreased exponentially with depth, reducing to e^{-1} of the surface value at a depth of around 140 m, and the jet was estimated to contain an offshore flux of about 10^6 m^3/s. These features are not inconsistent with the present observations. The *e*-folding depth of the offshore flow recorded at station E6 (Fig. 10) was around 100 m; through section A the alongshore flow showed an *e*-folding depth of about 130 m. The vertical shear in the upper layers is comparable off Oregon and Oman, having values in the range $1–2 \times 10^{-2}$ s^{-1}. Flament *et al.* (1985) found that the structure of a cold filament varied considerably over a time scale of 1–4 days, this is compatible with our observations of the variability in the offshore jet originally recorded along section E (Figs. 9–10) and then during the return to Muscat (Fig. 11). The horizontal scale of features at the two locations may be expected to differ since typical values for the internal Rossby radius off Oregon and Oman are 13 km and 27 km, respectively, the difference in the two scales being mainly due to the variation in latitude between the two areas.

With only 10 days of ship time, the cruise which started and ended in Muscat in the Gulf of Oman was limited in its objectives. Very little previous work has been done in these waters and we know of no direct current measurements made with *in situ* moorings and self recording current meters. Model studies, such as those of Luther and O'Brien (1985), can give some insight into the processes involved, but certain complexities—in particular those involving the interaction between the coastal flow and the Gulf of Oman—will benefit from further observational effort.

Acknowledgments. This work was supported by the Council for the Conservation of the Environment and Water Resources of the Sultanate of Oman. We thank the officers and crew of the RRS *Charles Darwin*, and L. M. L. Hubbard, P. Boyd, J. P. Johnston and P. McArdle for assistance during the collection of data at sea. Mr A. Mejia-Trejo helped with the processing of the FSU wind data (supplied by Prof. J. J. O'Brien and Dr D. Legler) and with the ship drift archive.

REFERENCES

Admiralty Pilot. 1967. Persian Gulf Pilot. Hydrographer of the Navy, London, 372 pp.

Bruce, J. G. 1974. Some details of upwelling off the Somali and Arabian coasts. J. Mar. Res., *32,* 419–423.

Fieux, M. 1975. Establissement de la mousson de Sud-Ouest en mer d'Arabie. C. R. Acad. Sc. Paris, *281,* 563–566.

Fieux, M. and H. Stommel. 1977. Onset of the southwest monsoon over the Arabian Sea from marine reports of surface winds: structure and variability. Mon. Weath. Rev., *105,* 231–236.
Flament, P., L. Armi and L. Washburn. 1985. The evolving structure of an upwelling filament. J. Geophys. Res., *90,* 765–11, 778.
Gregory, S. 1988. El Nino years and the spatial pattern of drought over India, 1901–1970, *in* Recent Climatic Change: A Regional Approach, S. Gregory, ed., Belhaven Press, 226–236.
Huyer, A. and P. M. Kosro. 1987. Mesoscale surveys over the shelf and slope in the upwelling region near Point Arena, California. J. Geophys. Res., *92,* 1655–1681.
Knox, R. A. and D. L. T. Anderson. 1985. Recent advances in the study of the low-latitude ocean circulation. Prog. Oceanogr., *14,* 259–317.
Kosro, P. M. 1987. Structure of the coastal current field off northern California during the coastal ocean dynamics experiment. J. Geophys. Res., *92,* 1637–1654.
Leetmaa, A., D. R. Quadfasel and D. Wilson. 1982. Development of the flow field during the onset of the Somali Current, 1979. J. Phys. Oceanogr., *12,* 1325–1342.
Legler, D. M., I. M. Navon and J. J. O'Brien. 1989. Objective analysis of pseudo-stress over the Indian Ocean using a direct-minimization approach. Mon. Weath. Rev., *117,* 709–720.
Luther, M. E. and J. O'Brien. 1985. A model of the seasonal circulation in the Arabian Sea forced by observed winds. Prog. Oceanogr., *14,* 353–385.
Qasim, S. Z. 1982. Oceanography of the northern Arabian Sea. Deep-Sea Res., *29,* 1041–1068.
Savidge, G., A. J. Elliott and L. M. L. Hubbard. 1990. The upwelling off Oman during summer 1987. Prog. Oceanogr., (submitted).
Schott, F. 1983. Monsoon response of the Somali Current and associated upwelling. Prog. Oceanogr., *12,* 357–381.
Smith, R. L. and J. S. Bottero. 1977. On upwelling in the Arabian Sea, *in* A Voyage of Discovery, M. Angel, ed., Pergamon Press, 291–304.
Warren, B. A., H. Stommel and J. C. Swallow. 1966. Water masses and patterns of flow in the Somali Basin during the southwest monsoon of 1964. Deep-Sea Res., *13,* 825–860.
Weaks, M. L. 1983. Satellite image of the month, Arabian Sea upwelling. Oceanog. Mon. Summ., *3,* 13.

Received *22 August, 1989;* revised: *23 January, 1990.*